



Dynamic MicroRNA Expression Profiles During Embryonic Development Provide Novel Insights Into Cardiac *Sinus Venosus*/Inflow Tract Differentiation

Carlos Garcia-Padilla^{1,2†}, Angel Dueñas^{1,2†}, Diego Franco^{2,3}, Virginio Garcia-Lopez¹, Amelia Aranega^{2,3}, Virginio Garcia-Martinez¹ and Carmen Lopez-Sanchez^{1*}

¹Department of Human Anatomy and Embryology, Faculty of Medicine, Institute of Molecular Pathology Biomarkers, University of Extremadura, Badajoz, Spain, ²Department of Experimental Biology, University of Jaen, Jaen, Spain, ³Fundación Medina, Granada, Spain

OPEN ACCESS

Edited by:

Rosa Barrio,
CIC bioGUNE, Spain

Reviewed by:

Marina Campione,
National Research Council (CNR), Italy
Raquel P. Andrade,
Universidade do Algarve, Portugal

*Correspondence:

Carmen Lopez-Sanchez
clopez@unex.es

[†]These authors have contributed
equally to this work and share first
authorship

Specialty section:

This article was submitted to
Morphogenesis and Patterning,
a section of the journal
Frontiers in Cell and Developmental
Biology

Received: 31 August 2021

Accepted: 16 December 2021

Published: 11 January 2022

Citation:

Garcia-Padilla C, Dueñas A, Franco D,
Garcia-Lopez V, Aranega A,
Garcia-Martinez V and
Lopez-Sanchez C (2022) Dynamic
MicroRNA Expression Profiles During
Embryonic Development Provide
Novel Insights Into Cardiac Sinus
Venosus/Inflow Tract Differentiation.
Front. Cell Dev. Biol. 9:767954.
doi: 10.3389/fcell.2021.767954

MicroRNAs have been explored in different organisms and are involved as molecular switches modulating cellular specification and differentiation during the embryonic development, including the cardiovascular system. In this study, we analyze the expression profiles of different microRNAs during early cardiac development. By using whole mount *in situ* hybridization in developing chick embryos, with microRNA-specific LNA probes, we carried out a detailed study of miR-23b, miR-130a, miR-106a, and miR-100 expression during early stages of embryogenesis (HH3 to HH17). We also correlated those findings with putative microRNA target genes by means of mirWalk and TargetScan analyses. Our results demonstrate a dynamic expression pattern in cardiac precursor cells from the primitive streak to the cardiac looping stages for miR-23b, miR-130a, and miR-106a. Additionally, miR-100 is later detectable during cardiac looping stages (HH15-17). Interestingly, the *sinus venosus*/inflow tract was shown to be the most representative cardiac area for the convergent expression of the four microRNAs. Through *in silico* analysis we revealed that distinct Hox family members are predicted to be targeted by the above microRNAs. We also identified expression of several Hox genes in the *sinus venosus* at stages HH11 and HH15. In addition, by means of gain-of-function experiments both in cardiomyoblasts and *sinus venosus* explants, we demonstrated the modulation of the different Hox clusters, Hoxa, Hoxb, Hoxc, and Hoxd genes, by these microRNAs. Furthermore, we correlated the negative modulation of several Hox genes, such as Hoxa3, Hoxa4, Hoxa5, Hoxc6, or Hoxd4. Finally, we demonstrated through a dual luciferase assay that Hoxa1 is targeted by miR-130a and Hoxa4 is targeted by both miR-23b and miR-106a, supporting a possible role of these microRNAs in Hox gene modulation during differentiation and compartmentalization of the posterior structures of the developing venous pole of the heart.

Keywords: heart development, microRNAs, expression profiles, Hox genes, sinus venosus, inflow tract

INTRODUCTION

During chick gastrulation (stage HH3; Hamburger and Hamilton, 1951, 1992) the primitive streak precardiac cells invaginate and migrate anterolaterally to form the precardiac mesoderm, between the ectoderm and the inductive adjacent endoderm (Garcia-Martinez and Schoenwolf, 1993; Schultheiss et al., 1995; Garcia-Martinez et al., 1997; Redkar et al., 2001; Lopez-Sanchez et al., 2001, 2009, 2018), at both sides of the embryo (stages HH5-7), determining the first heart field (FHF; Harvey, 2002). Subsequently, this field will form the primitive endocardial tubes (stage HH8), which in the midline fuse into a single heart tube (stage HH10), structured into the endocardial and myocardial layers (Lopez-Sanchez and Garcia-Martinez 2011). Later on, a progenitor population originating from the adjacent pharyngeal mesoderm, the secondary heart field (SHF; Buckingham et al., 2005), will contribute to further cardiac development, giving rise to the dorsal *mesocardium*, as well as the posterior (venous) and anterior (arterial) heart poles, differentiating the inflow (IFT) and outflow tracts (OFT), respectively (Waldo et al., 2005; Abu-Issa and Kirby 2008; van den Berg et al., 2009; Camp et al., 2012; Zaffran and Kelly, 2012; De Bono et al., 2018a). The IFT, a relevant segment in the sinoatrial node formation, develops from a restricted set of cardiomyocytes located in the *sinus venosus* (SV). Furthermore, the outer surface of the SV gives rise to the proepicardium—epicardial primordium—development (Christoffels et al., 2006; van Wijk et al., 2009, 2018; Mommersteeg et al., 2010; Carmona et al., 2018).

A complex network of signaling pathways and transcriptional factors is required to regulate early cardiac development. In this sense, the FGF, TGF, and Wnt pathways, among others, have been widely involved in early cardiogenesis. In particular, within this signaling network, retinoic acid (RA) has been shown to pattern the SHF (Hochgreb et al., 2003; Stefanovic and Zaffran, 2017). RA signaling is required for SHF differentiation, modulating the expression of specific marker genes, including *Fgf8*, *Fgf10*, and *Tbx1* (Ryckebusch et al., 2008; Sirbu et al., 2008; De Bono et al., 2018b). Previous genetic lineage analyses in mice have revealed that Homeobox (Hox) gene expressions—*Hoxa1*, *Hoxa3*, and *Hoxb1*—define distinct domains and sub-domains within the SHF (Bertrand et al., 2011). Thus, *Hoxa1*- and *Hoxb1*-expressing progenitor cells contribute to both cardiac poles' development, the IFT and the inferior wall of the OFT (Bertrand et al., 2011; Lescroart and Zaffran, 2018; Stefanovic et al., 2020).

Due to the fact that microRNAs represent a novel layer of complexity in the regulatory networks controlling gene expression, cell specification, and differentiation (Choi et al., 2013; Rajabi et al., 2020), this subclass of non-coding RNAs has been widely analyzed by its relevant role in cardiac development. Previous studies have provided evidence on the differential expression of several microRNAs contributing to cardiac fate specification and maintenance of cardiac progenitors during development (Chinchilla et al., 2011; Cao et al., 2012; Lopez-Sanchez et al., 2015a; Lopez-Sanchez et al., 2015b; Yan and Jiao 2016; Kalayinia et al., 2021). Some

microRNA expressions, such as those of miR-125b, miR-142-3p, and miR-137, have also been referenced in the SV/IFT (Darnell et al., 2006).

In order to shed light on microRNAs and their role during early cardiac development, in this work, we analyze the expression pattern of miR-23b, miR-130a, miR-106a, and miR-100, from early stages of embryogenesis (HH3 to HH17). Although these microRNAs have been previously involved in cardiac structural and functional characteristics (Sucharov et al., 2008; Thum et al., 2008; Aguirre et al., 2014; Guan et al., 2016; Boureima Oumarou et al., 2019), their roles during cardiac development have still not been assessed. Our results show a common expression of these microRNAs in specific cardiac structures, the SV/IFT being the most representative cardiac area for their convergent expression. Also, we have correlated these findings with several Hox family members revealed as targets of these microRNAs by means of mirWalk and TargetScan analyses. Furthermore, we have identified that several Hox genes targeted by these microRNAs are expressed in the HH11 and HH15 *sinus venosus*. Finally, by using *in vitro* microRNA gain-of-function experiments on cardiomyoblasts derived from undifferentiated H9c2 cells, together with an analysis of chicken *sinus venosus* explants, we have shown in this study the specific relevance of distinct microRNAs in Hox gene modulation, suggesting a possible molecular role in the differentiation and/or compartmentalization of the developing venous pole of the heart.

RESULTS

Expression Profile of miR-23b, miR-130a, miR-106a, and miR-100 During Early Embryonic Development

In this work, we have analyzed the expression profile of miR-23b, miR-130a, miR-106a, and miR-100 during early chicken embryonic development (Figures 1, 2), starting at early gastrulation stages through the formation of the early cardiac looped stages, from HH3 to HH17.

From early stages of development, miR-23b (Figure 1A) extends along the primitive streak (HH3). Later, this expression expands to the precardiac mesoderm and the underlying endoderm at both sides of the embryo and contributes to the formation of the first heart field (HH5), maintaining its expression in both primitive endocardial tubes (HH8). As shown in HH9-10, during cardiac tube formation, this expression is progressively restricted to the inflow tract. Noticeably, during early cardiac looping (HH11), miR-23b is expressed in both inflow and outflow tracts, subsequently being more evident on the dorsal surface of the cardiac *sinus venosus* and the dorsal mesocardium (HH14).

We have previously described that miR-130a starts expressing at the primitive streak stage (HH3), followed by an expansion toward both sides of the mesodermal and endodermal layers of the embryo (HH4). From stage HH5 onward, miR-130a is progressively restricted to the precardiac mesoderm and its

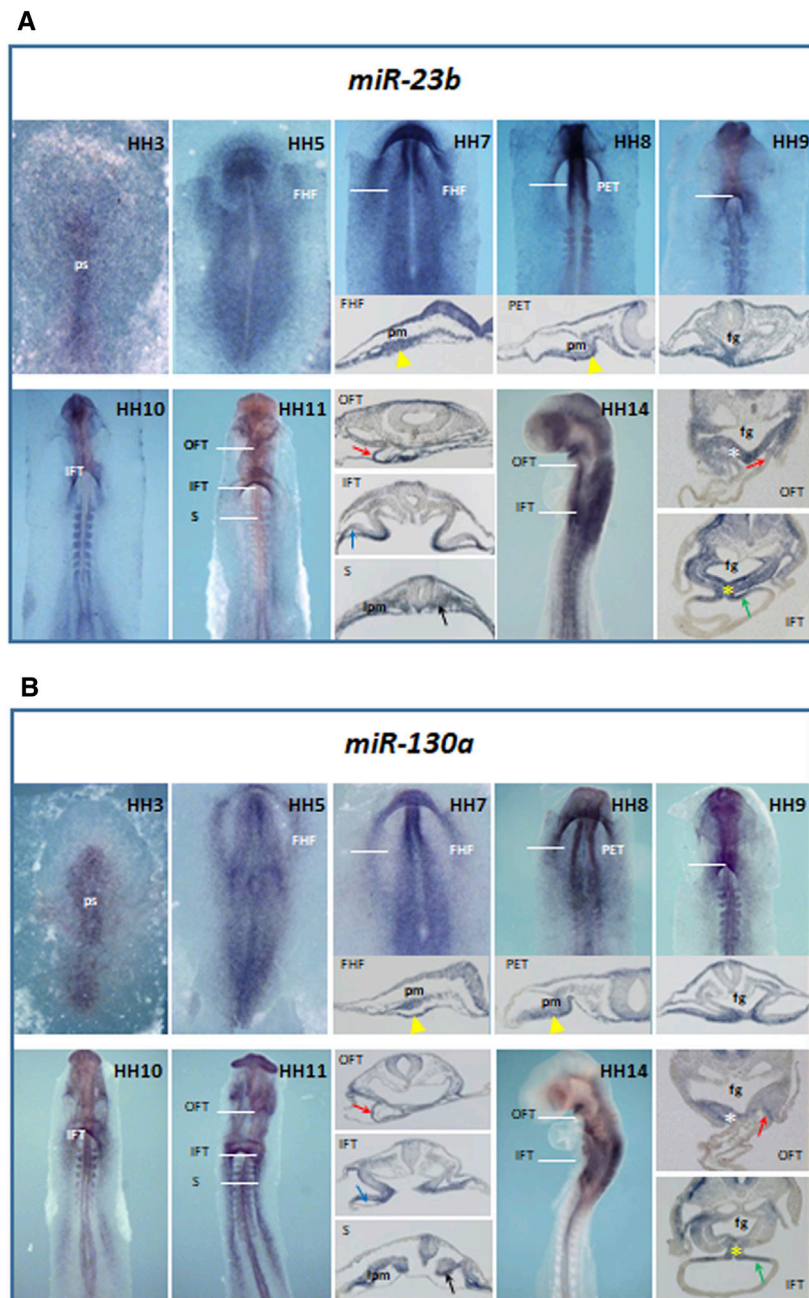


FIGURE 1 | Whole-mount ISH analysis of miR-23b (A), miR-130a (B), miR-106a (C), and miR-100 (D) during chick embryo cardiac development, from HH3 through HH14. White lines indicate the transverse section levels of selected embryos: FHF, first heart field; PET, primitive endocardial tube; IFT, inflow tract; OFT, outflow tract and S, somite level. Note their expressions in the primitive streak (ps), precardiac mesoderm (pm), adjacent endoderm to precardiac mesoderm (yellow arrowhead), OFT (red arrow), dorsal surface of *sinus venosus* (green arrow), dorsal mesocardium (yellow asterisk), and vitelline vein (blue arrow); as well as in the foregut (fg), pharyngeal mesoderm (white asterisk), lateral plate mesoderm (lpm), and somites (black arrow) for miR-23b (A), miR-130a (B), and miR-106a (C). Just from stage HH15 is observable miR-100 expression (D) in cardiac structures. V, ventricle.

underlying endoderm, subsequently expressing in both primitive endocardial tubes (Lopez-Sanchez et al., 2015a). One of the novelties of this study lies in the identification of miR-130a expression during primitive cardiac tube formation (Figure 1B), specifically in the dorsal mesocardium and the

dorsal wall of the cardiac *sinus venosus* (HH9-14), as well as in the outflow tract.

During early stages of development, miR-106a (Figure 1C) shows a broad expression in the embryo, sharper in the primitive streak (HH3). Afterward, it expresses homogeneously throughout

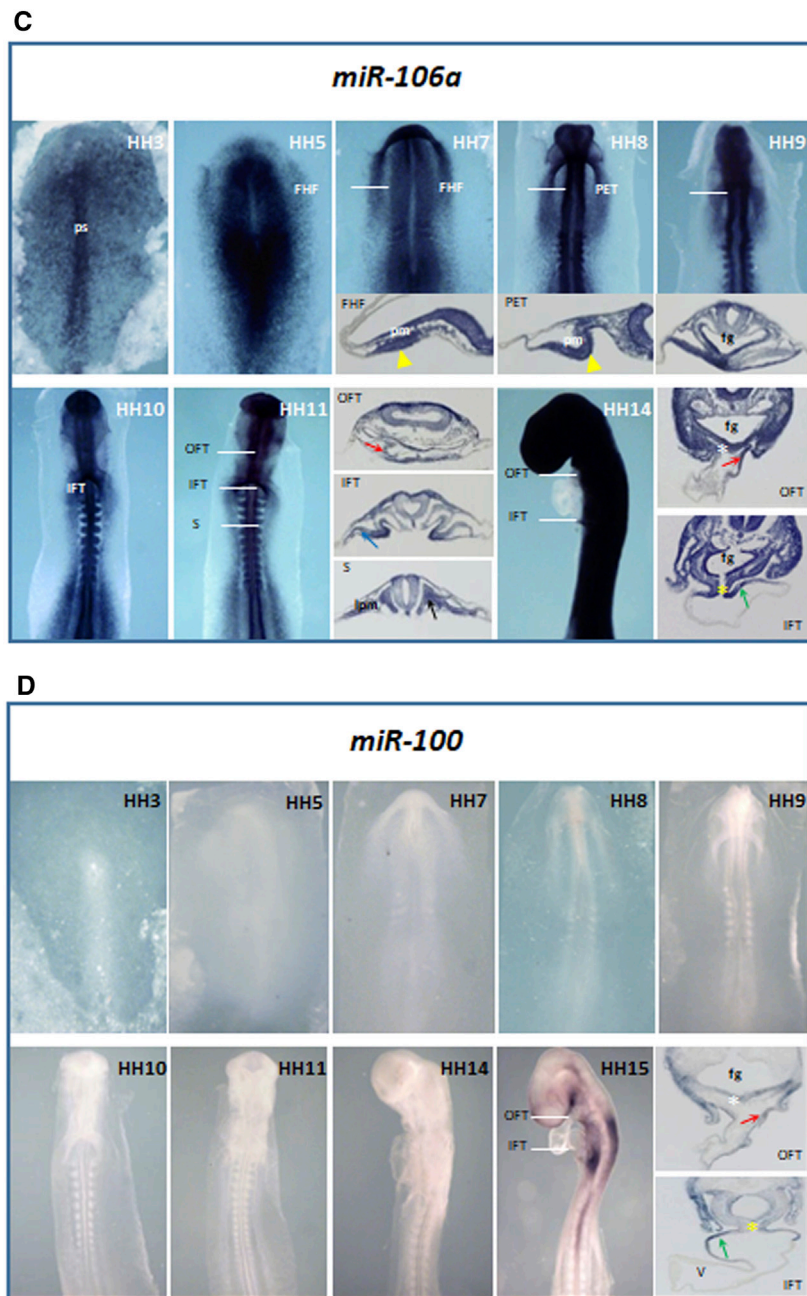


FIGURE 1 | (Continued).

the embryo (HH5–13), excluding the extraembryonic tissue. Although this expression covers all the heart regions and derivatives at early stages (HH8–11), it is restricted to the dorsal mesocardium and the inflow and outflow tracts at later stages (HH14). The signal stays homogeneously strong in the remaining embryo, except in the developing cardiac chambers.

Additionally, we have observed the expression of the microRNAs mentioned above in somites and the lateral plate mesoderm, among others (Figures 1A–C).

Unlike miR-23b, miR-130a, and miR-106a, the expression of miR-100 starts at the HH15 stage, being evident on the dorsal surface of the inflow tract and in the dorsal mesocardium and outflow tract (Figure 1D).

During cardiac looping stages (HH15–17), the four microRNAs analyzed (Figure 2) are expressed in the lateral–dorsal wall of the outflow tract and foregut, being evident in the dorsal wall of the inflow tract and the dorsal mesocardium. Interestingly, in these stages, all these microRNAs

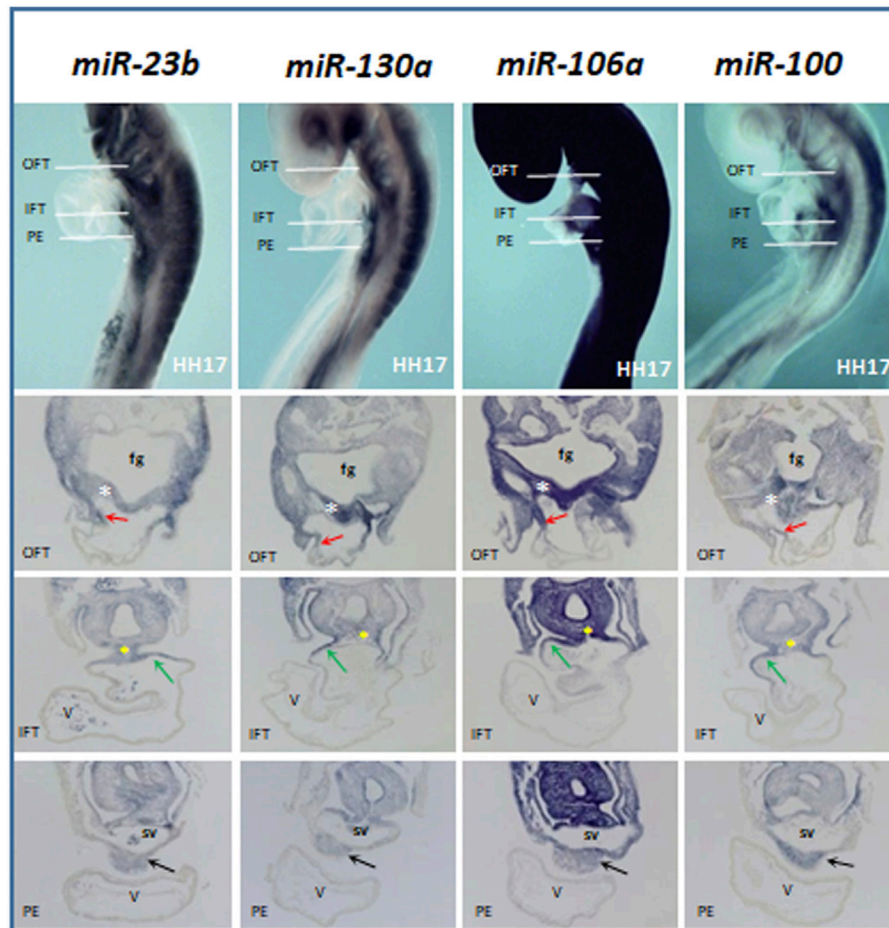


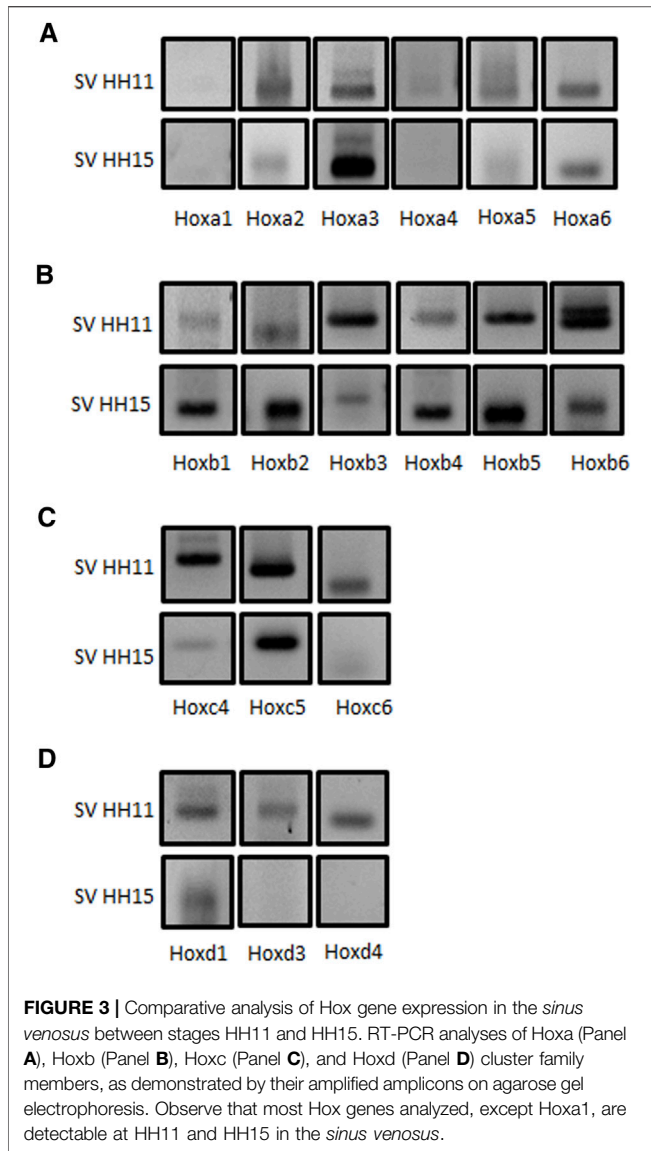
FIGURE 2 | Comparative whole-mount ISH analysis of miR-23b, miR-130a, miR-106a, and miR-100 expression profiles at stage HH17. The transverse section levels are indicated with white lines: OFT, outflow tract; IFT, inflow tract, and PE, proepicardium. Note their expressions in the lateral–dorsal wall of the OFT (red arrow), foregut (fg), dorsal wall of the IFT (green arrow), dorsal mesocardium (yellow asterisk), and proepicardium (black arrow). White asterisk, pharyngeal mesoderm; V, ventricle; sv, *sinus venosus*.

show a marked expression in the proepicardium, which is formed at the cardiac inflow region, both coming from a common progenitor pool (van Wijk et al., 2009, 2018).

Hox Cluster Family Members Are Differentially Modulated by miR-23b, miR-130a, miR-106a, and miR-100

Modulation by multiple microRNAs within the same pathway—and even common targets—has been widely reported (Wu et al., 2010; Shu et al., 2017). Since those microRNAs analyzed in this study are particularly expressed in the cardiac inflow tract at early developing stages, we have considered that they could recognize common targets likely involved in the differentiation processes of this segment. Several gene families and transcription factors are important to establish compartmentalization of the embryo, especially during early stages of development. In this sense, Hox gene families have gained pivotal relevance in the last 3 decades.

Those genes are broadly conserved during evolution, and their roles to shape the body of the embryo have been widely described in multiple species (Roux and Zaffran, 2016; Lescroart and Zaffran, 2018). In addition, expression of Hox genes in the cardiovascular system is rather restricted, mostly confined to the posterior SHF-derived venous pole of the heart. We therefore explored the expression profile of all cranially expressed Hox genes, including all paralogues (Hoxa to Hoxd) from one to six in the chicken cardiac *sinus venosus* at stages HH11 and HH15 (Figure 3). From our data, most of these Hox genes were detected in the *sinus venosus* at stages HH11 and HH15, except for Hoxa1 (Figure 3A). In addition, we observed that Hoxa2, Hoxa4, and Hoxa5 (Figure 3A), Hoxb3 and Hoxb6 (Figure 3B), Hoxc4 and Hoxc6 (Figure 3C), and Hoxd1, Hoxd3, and Hoxd4 (Figure 3D) display well-marked expression at stage HH11 compared to HH15. On the other hand, Hoxa3 (Figure 3A), Hoxb1, Hoxb2, Hoxb4, and Hoxb5 (Figure 3B) showed an intense expression at HH15. Finally, Hoxa6 and Hoxc5 presented a similar expression at both stages (Figures 3A,C).

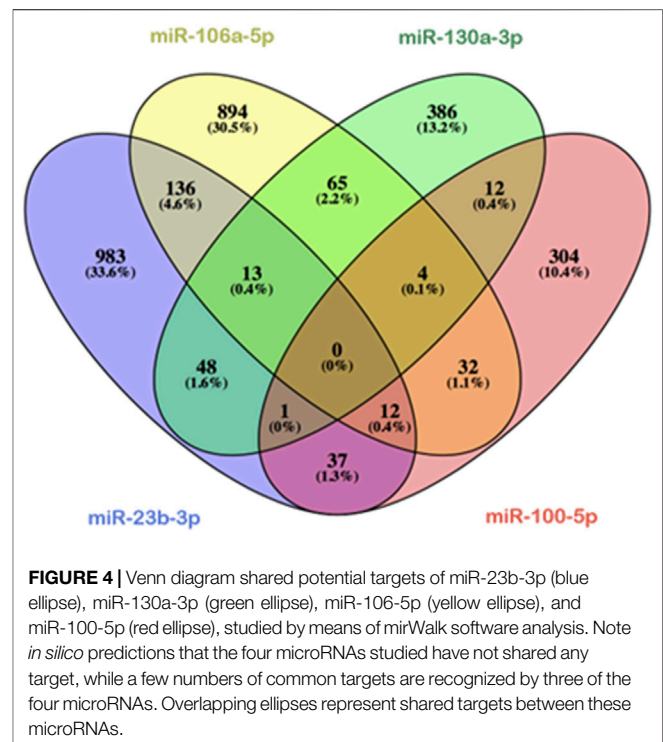


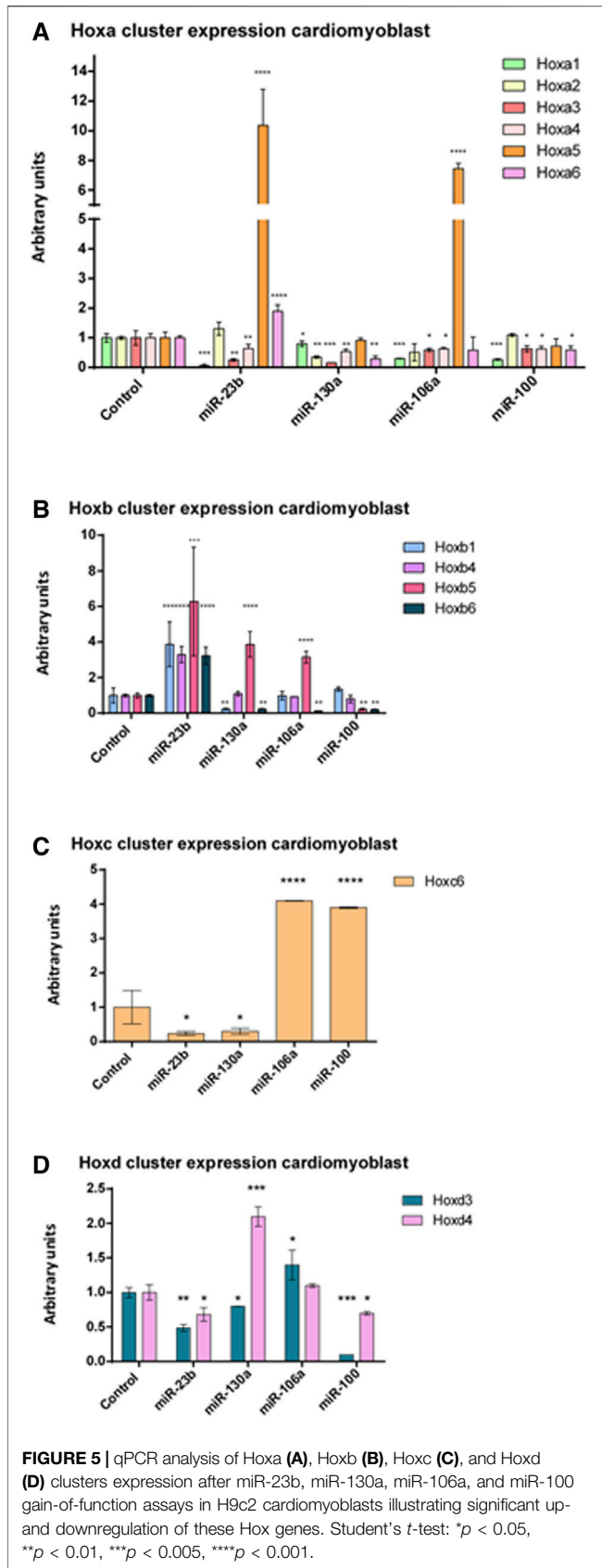
Since several Hox genes are expressed at stages HH11 and HH15, we considered in this study the possibility that microRNAs under analysis could be recognizing the 3'UTRs of the distinct Hox genes and thus modulating their expression. By using mirWalk (Sticht et al., 2018) and TargetScan softwares, we analyzed *in silico* those common targets shared by miR-23b, miR-130a, miR-106a, and miR-100. It is observed that these four microRNAs do not share any targets simultaneously, as shown in Figure 4. On the other hand, all Hox genes are recognized by at least one of these microRNAs, except Hoxa6 (Supplementary Table S1).

It is to note that H9c2 cardiomyoblasts can be differentiated into cardiomyocytes by administrating retinoic acid (RA) to the culture medium when cells reach a high degree of confluence (Branco et al., 2015). Our expression analyses of Nkx2.5—an early cardiogenic marker—and cardiac troponin T (cTnT)—a late differentiation marker—corroborated that there are differences

between H9c2 cardiomyoblasts and cardiomyocytes (Supplementary Figure S1). To assess the possible role of these microRNAs as Hox gene modulators, we performed microRNA gain-of-function assays in cardiomyoblasts (Supplementary Figure S2). As observed in Figure 5 and summarized in Table 1, after gain-of-function experiments in cardiomyoblasts, Hoxa1, Hoxa3, and Hoxa4 were repressed by the four microRNAs studied. Also, Hoxa2 and Hoxa5 were inhibited by miR-130a, and Hoxa6 was downregulated by miR-130a and miR-100. On the other hand, Hoxa5 was significantly upregulated by miR-23b and miR-106a administration. Hoxa6 was also upregulated by miR-23b (Figure 5A). With respect to the Hoxb cluster (Figure 5B, Table 1), different Hox genes were repressed by their respective microRNAs (Hoxb1/miR-130a; Hoxb5/miR-100 and Hoxb6 by miR-130a, miR-106a and miR-100). On the other hand, Hoxb1, Hoxb4, Hoxb5, and Hoxb6 were significantly upregulated by miR-23b. Hoxb5 was also upregulated by miR-130a and miR-106a. Hoxb2 and Hoxb3 were not detected in H9c2 cardiomyoblasts. Within the Hoxc cluster, only Hoxc6 expression was observed, showing a downregulation by miR-23b and miR-130a and upregulation by miR-106a and miR-100 (Figure 5C, Table 1). Finally, in reference to the Hoxd cluster (Figure 5D, Table 1), Hoxd3 and Hoxd4 were repressed by miR-23b and miR-100, and also, Hoxd3 was downregulated by miR-130a. In contrast, Hoxd3 and Hoxd4 were upregulated by miR-106a and miR-130a, respectively. Hoxd1 expression was not detected in H9c2 cardiomyoblasts.

Subsequently, in order to determine the modulation of Hox genes by these microRNAs in the developing venous pole of the heart, we performed gain-of-function experiments in *sinus*





venosus explants, at stages HH11 and HH15 (Supplementary Figure S3). Figure 6 and Tables 2, 3 summarize our data, showing that Hoxa3 was downregulated by miR-23b, miR-106a, and miR-100 at stage HH11. Hoxa4 was downregulated by miR-130a and miR-100 at stage HH11 and by miR-23b, miR-106, and miR-100 at HH15 (Figures 6A, B). These data are in line with the results obtained in our gain-of-function experiments in cardiomyoblasts. Additionally, Hoxa5 was repressed by miR-23b, miR-106a, and miR-100 at stage HH11, while it was downregulated by miR-23b, miR-130a, and miR-106a at HH15. Also, Hoxa2 was repressed by miR-130a and miR-106a at HH15, suggesting their involvement in further stages of *sinus venosus* formation. On the other hand, the downregulation of Hoxb6 by miR-106a both in *sinus venosus* explants at HH11 and cardiomyoblasts would suggest a participation in early differentiation. As observed in Figures 6C, D, Hoxb1 and Hoxb4 were not detected in these experiments. Coinciding with the results obtained in cardiomyoblasts, Hoxc6 was downregulated by miR-23b and miR-130a at stage HH15 (Figure 6F) and Hoxd4 was repressed by miR-23b and miR-100 at HH11 (Figure 6G).

Since Hoxa1 and Hoxa4 expressions were modulated negatively by those microRNAs analyzed *in vitro* and given that their 3'UTR harbor multiple seed sequences for these microRNAs, we performed dual luciferase biochemical assays to determine whether miR-23b, miR-130a, miR-106a, and miR-100 could directly target either Hoxa4 or Hoxa1 3'UTRs (Figure 7). Our data demonstrated that miR-130a could not interact directly with Hoxa4 3'UTR (Figure 7A), which is in agreement with the fact that this microRNA is not predicted either by mirWalk or TargetScan. Interestingly, transfection with miR-106a and miR-23b significantly decreased Hox4 luciferase levels with respect to control samples (Figures 7B, C), in line with mirWalk predictions (Supplementary Table S1), thus proving a direct interaction between those two microRNAs and Hoxa4 3'UTR. As for Hoxa1 3'UTR (Figures 7D–F), only miR-130a reduced luciferase levels with respect to the control, thus suggesting an indirect repression exerted by miR-23b, miR-106a, and miR-100 on this gene.

DISCUSSION

Previous studies have demonstrated that a single microRNA may be a crucial regulator both in cardiac development and function. Imbalanced microRNA expression in the progenitor cells of the developing heart might cause congenital and/or structural defects, including altered cell migration and proliferation, as well as inappropriate cell type specification (Pang et al., 2019; Kalayinia et al., 2021). In particular, it has been reported that: 1) miR-23b is upregulated in cardiac hypertrophy, and its overexpression in cardiomyocytes *in vitro* is sufficient to promote hypertrophic growth (Thum et al., 2008; Boureima Oumarou et al., 2019); 2) miR-130a is required for adequate proliferation of cardiac progenitors (Kim et al., 2009), supported by gain-of-function murine experiments, leading to cardiomyocyte proliferation defects as ventricular hypoplasia; 3) miR-106a is

TABLE 1 | Hox genes modulated by microRNAs in cardiomyoblasts.

	Hoxa1	Hoxa2	Hoxa3	Hoxa4	Hoxa5	Hoxa6	Hoxb1	Hoxb4	Hoxb5	Hoxb6	Hoxc6	Hoxd3	Hoxd4
miR-23b	↓	—	↓	↓	↑	↑	↑	↑	↑	↑	↓	↓	↓
miR-130a	↓	↓	↓	↓	↓	↓	↓	—	↑	↓	↓	↓	↑
miR-106a	↓	—	↓	↓	↑	—	—	—	↑	↓	↑	↑	—
miR-100	↓	—	↓	↓	—	↓	—	—	↓	↓	↑	↓	↓

Diagram illustrating Hox genes modulation exerted by miR-23b, miR-130a, miR-106a and miR-100 after gain-of-function assays in cardiomyoblast cell line (obtained from Figure 5). Green arrows: upregulated. Red arrows: downregulated. Black lines: Do not regulate.

significantly upregulated in cardiac hypertrophy, as demonstrated by *in vivo* and *in vitro* analyses (Guan et al., 2016); and 4) although miR-100 function is not relevant to hypertrophic gene expression, its role in cardiac regeneration has been widely demonstrated in zebrafish and mice, and it also plays specific roles in adult isoform cardiac gene regulation (Tarantino et al., 2010; Aguirre et al., 2014).

Since these microRNAs have proved significant in cardiac structural and functional features, we will proceed to discuss their relevance during cardiac development. Previously, the expression profile of miR-23b has been identified in the cardiac tissue of fetal mice from E12.5 to E18.5 (Cao et al., 2012). Also, miR-23b expression has been observed in developing chicks, although restricted to the atrium and the dorsal aorta, since stage HH22. On the other hand, a widespread expression of miR-130a, miR-106a, and miR-100 has been described (Darnell et al., 2006), although cardiac expression of these microRNAs has not been previously described. In our study, we carried out a detailed analysis of miR-23b, miR-130a, miR-106a, and miR-100 expression profiles, from early gastrulation stages to the formation of the early cardiac looping stage. Our results reveal miR-23b, miR-130a, and miR-106a expressions in the primitive streak and the first heart field, maintaining their expressions in both primitive endocardial tubes and cardiac tube formation. In addition, miR-100 expression is observed during cardiac looping stages. Subsequently, these four microRNAs show common expression in specific cardiac structures, including inflow and outflow tracts, as well as the dorsal mesocardium and the proepicardium. This is the first time that the cardiac expression profiles of these four microRNAs have been described, suggesting that they could play crucial roles in multiple cardiac development processes from early stages.

In our study, we show that numerous Hox genes are expressed in the *sinus venosus* at stages HH11 and HH15. These data are relevant since, to date, only the expression of a few Hox genes—Hoxa1, Hoxa3, Hoxa4, Hoxb1, and Hoxb4—has been demonstrated in different species (Searcy and Yutzey, 1998; Makki and Capecchi, 2010; Bertrand et al., 2011; Barak et al., 2012; Roux et al., 2015; Lescroart and Zaffran, 2018; Stefanovic et al., 2020). We have subsequently explored the possibility that those microRNAs studied by ISH, the expression of which is particularly observed in the *sinus venosus*, could recognize 3'UTRs regions of the Hox genes and modulate their expression. Based on *in silico* analysis, we observe that one or more of the microRNAs under study recognized all cranially expressed Hox genes, including all paralogues (Hoxa to Hoxd) from 1 to 6, except Hoxa6. The potential modulation of Hox gene expression is confirmed by the results we obtained from *in vitro* assays in cardiomyoblasts and *ex vivo* assays in *sinus venosus* explants.

The role of retinoic acid (RA) in differentiation and morphogenesis of structures derived from the posterior segment of the heart tube has been widely described (Bertrand et al., 2011; De Bono et al., 2018b). Deficient RA synthesis results in cellular hypoplasia and, consequently, in morphogenetic defects in both the atrium

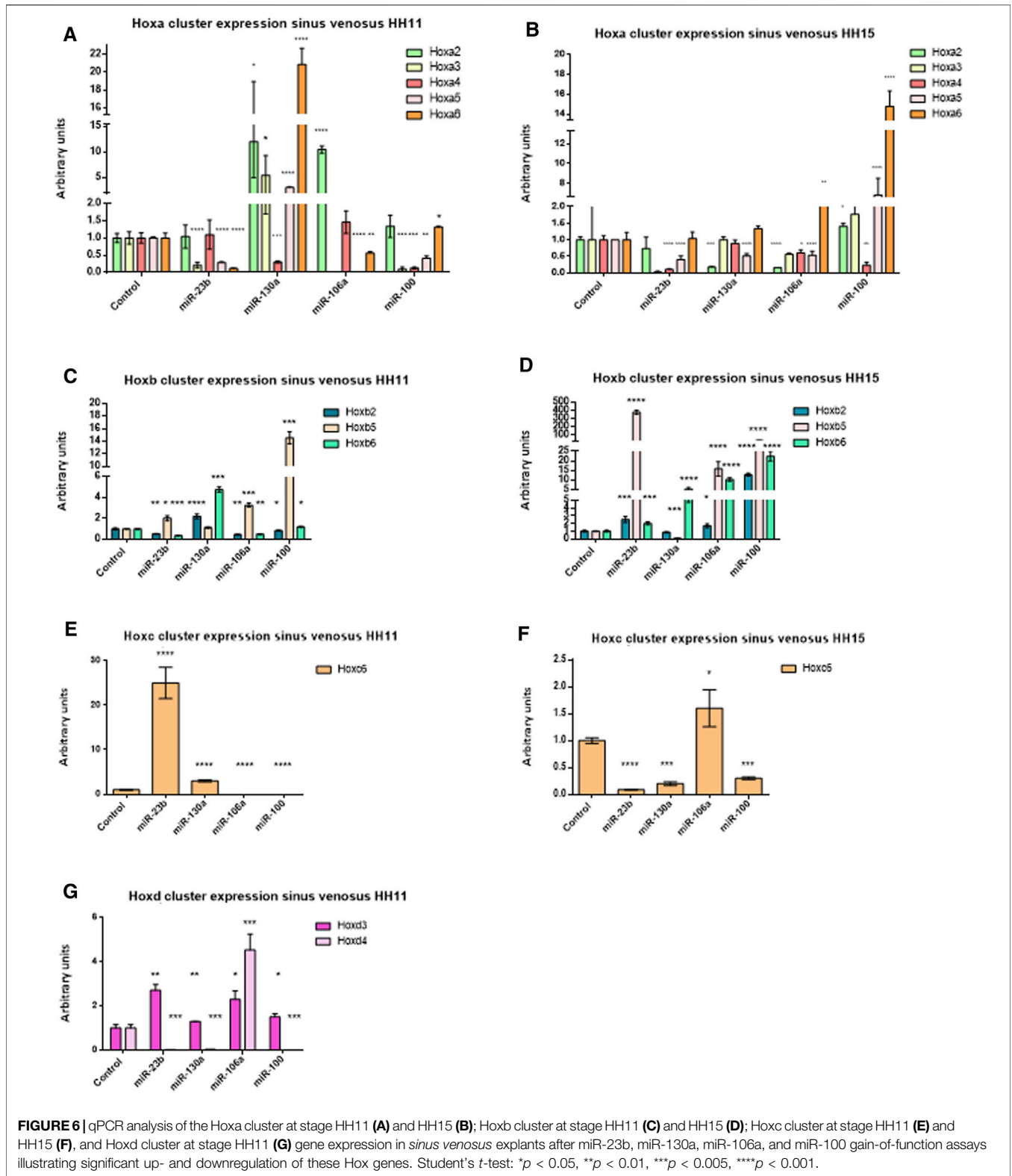


FIGURE 6 | qPCR analysis of the Hoxa cluster at stage HH11 (A) and HH15 (B); Hoxb cluster at stage HH11 (C) and HH15 (D); Hoxc cluster at stage HH11 (E) and HH15 (F), and Hoxd cluster at stage HH11 (G) gene expression in *sinus venosus* explants after miR-23b, miR-130a, miR-106a, and miR-100 gain-of-function assays illustrating significant up- and downregulation of these Hox genes. Student's *t*-test: **p* < 0.05, ***p* < 0.01, ****p* < 0.005, *****p* < 0.001.

TABLE 2 | Hox genes modulated by microRNAs in the *sinus venosus* at stage HH11.

	Hoxa2	Hoxa3	Hoxa4	Hoxa5	Hoxa6	Hoxb2	Hoxb5	Hoxb6	Hoxc6	Hoxd3	Hoxd4
miR-23b	—	↓	—	↓	↓	↓	↑	↓	↑	↑	↓
miR-130a	↑	↑	↓	↑	↑	↑	—	↑	↑	↑	↓
miR-106a	↑	↓	—	↓	↓	↓	↑	↓	↓	↑	↑
miR-100	—	↓	↓	↓	↑	↓	↑	↑	↓	↑	↓

Diagram illustrating Hox genes modulation exerted by miR-23b, miR-130a, miR-106a and miR-100 after gain-of-function assays in *sinus venosus* explants at stage HH11 (obtained from Figures 6A, C,E, G). Green arrows: upregulated. Red arrows: downregulated. Black lines: Do not regulate.

TABLE 3 | Hox genes modulated by microRNAs in the *sinus venosus* at stage HH15.

	Hoxa2	Hoxa3	Hoxa4	Hoxa5	Hoxa6	Hoxb2	Hoxb5	Hoxb6	Hoxc6	Hoxd3	Hoxd4
miR-23b	—	—	↓	↓	—	↑	↑	↑	↓	ND	ND
miR-130a	↓	—	—	↓	—	—	↓	↑	↓	ND	ND
miR-106a	↓	—	↓	↓	↑	↑	↑	↑	↑	ND	ND
miR-100	↑	—	↓	↑	↑	↑	↑	↑	↓	ND	ND

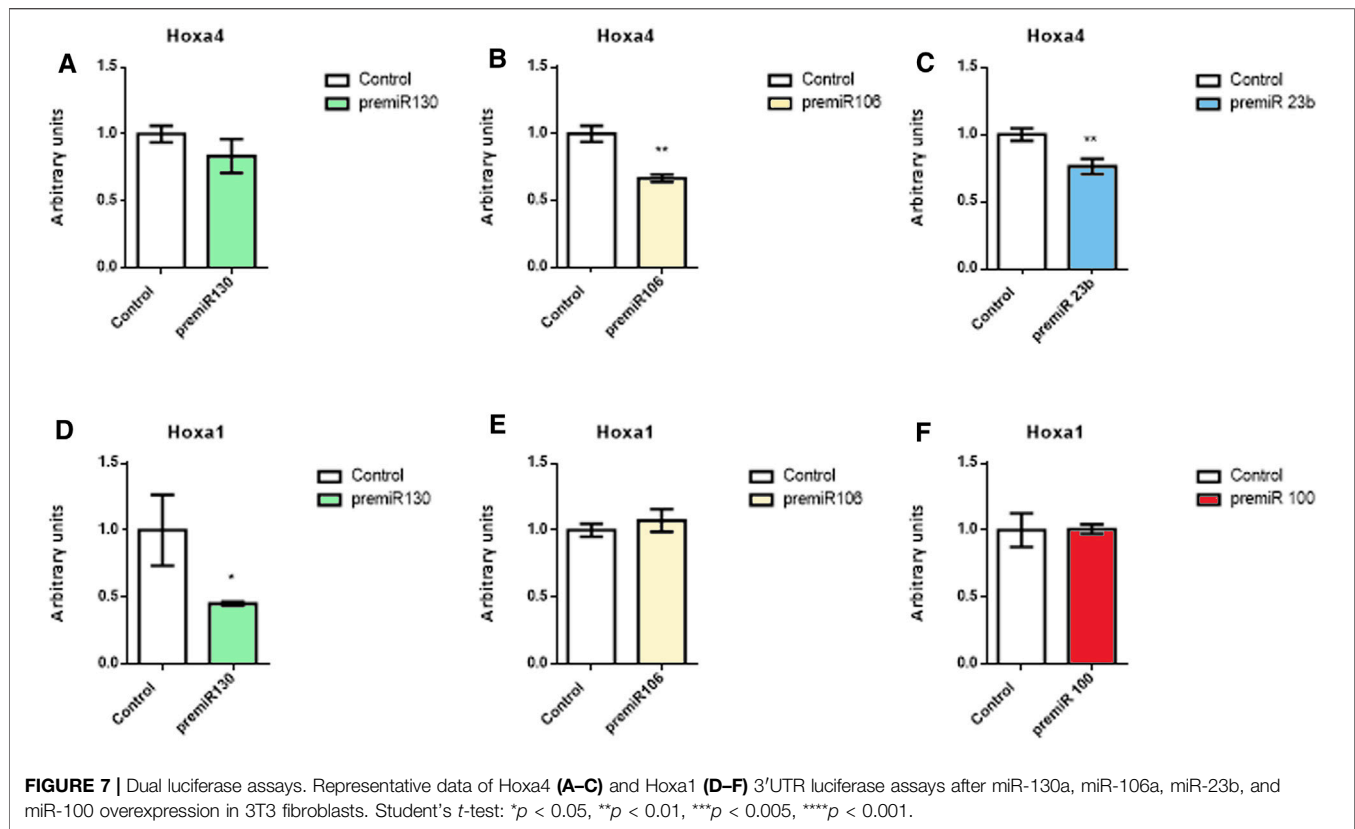
Diagram illustrating Hox genes modulation exerted by miR-23b, miR-130a, miR-106a and miR-100 after gain-of-function assays in *sinus venosus* explants at stage HH15 (obtained from Figures 6B, D, F). Green arrows: upregulated. Red arrows: downregulated. Black lines: Do not regulate. ND: no detectable.

and the *sinus venosus* (Niederreither et al., 1999, 2001). Interestingly, the administration of RA during mouse lung development is sufficient to induce Hoxa4 expression (Packer et al., 1998, 2000). Also, this gene has been recognized in many tissues as a potent inhibitor of cell mobility (Bhatlekar et al., 2017; Cheng et al., 2018). In our study, Hoxa4 provides an interesting example of a Hox gene downregulated by the microRNAs analyzed, as illustrated by both *in vitro* and *ex vivo* assays. In this context, it should be noted that the mobility of the cardiac progenitors is a dynamic and continuous determinant process during heart remodeling and conformation. Similarly, adequate cardiac physiological function requires certain cell subpopulation movement, not yet fully defined, from their origin to other cardiac regions. The repression of Hoxa4 that we observed in the *sinus venosus* at stages HH11 and HH15 reflects a much more complex mechanism, which may be responsible for cell mobility regulation of the different cardiac progenitors, likely involved in the developing venous pole of the heart. Although Hoxa4 modulation by means of microRNAs has not yet been described, some authors have demonstrated a negative modulation of Hoxa5 by miR-130a, after induction of

Hoxa5 by RA (Yang et al., 2013). Supporting these data, our luciferase assays reveal that Hoxa4 is repressed by miR-23b and miR-106a, as the consequence of a direct physical interaction exerted between these microRNAs and its 3'UTR region.

On the other hand, we observe that Hoxd3 is upregulated both in the cardiomyoblasts and the *sinus venosus* at stage HH11. Previous reports have pointed out that Hoxd3 is not expressed at later stages of cardiogenesis and also that treatment with RA is sufficient to repress its expression (Searcy and Yutzey, 1998), showing an opposite behavior to that of Hoxa4. In agreement with the above, in our study we observed that the expression of Hoxd3 is not detected in the *sinus venosus* at stage HH15. This fact could be a consequence of the specific restricted pattern of the microRNAs—miR23b, miR-130a, miR-106a, and miR-100—during this stage.

In summary, this study shows several novel findings in the field of cardiac development. Our data show a dynamic expression of miR-23b, miR-130a, miR-106a, and miR-100 from early stages of cardiogenesis. We also identify the expression of several Hox genes in the *sinus venosus* at stages HH11 and HH15. Noticeably, we observe that there



is a negative modulation of several Hox genes by microRNAs, both in cardiomyoblasts and *sinus venosus*. Finally, the convergent expression of these microRNAs regulating Hox gene expressions in the *sinus venosus*/inflow tract supports the hypothesis of a potential role in differentiation and compartmentalization of the cardiac venous pole.

MATERIALS AND METHODS

Whole-Mount LNA *In Situ* Hybridization (ISH) and Sectioning

Fertilized eggs (Granja Santa Isabel, Córdoba, Spain) were incubated at 38°C in forced-draft, humidified incubators. Embryos were collected at stages HH3 to HH17 (Hamburger and Hamilton, 1951, 1992; Lopez-Sanchez et al., 2005) and fixed overnight at 4°C in 4% PFA, dehydrated in methanol, and stored at –20°C. Embryos were processed for LNA-ISH following our previous procedure (Lopez-Sanchez et al., 2015a) using miR-23b, miR-130a, miR-106a, and miR-100 LNA-labeled microRNA probes (miRCURY LNA™ Detection probe 5'-DIG and 3'-DIG labeled, Exiqon), respectively.

For histology, embryos were dehydrated with an ethanol series, cleared in isopropanol, and processed for paraplast embedding, obtaining 15-µm transverse serial sections.

H9c2 Cell Culture and microRNAs Transfections

The H9c2 cell line (kindly provided by Dr. Paulo J. Oliveira, Coimbra, Portugal) was cultured in DMEM medium supplemented with 10% foetal bovine serum, 100 U/mL penicillin, and 100 µg/ml streptomycin in 100-cm² culture disks at 37°C in a humidified atmosphere of 5% CO₂. Cells were fed every 2–3 days. Two sub-cultured condition transfections were performed. Myoblast H9c2 was sub-cultured at 50–60% confluence while induced-cardiomyocyte H9c2 reached 80–90% confluence. H9c2 cells (6 × 10⁵ cells per well) were transfected with microRNA mimics for miR-23b, miR-130a, miR-106a, and miR-100 precursors (Thermo Fisher) as previously described (Branco et al., 2015).

Sinus Venosus Resection and microRNAs Transfections

Groups of embryos were collected at stages HH11 and HH15 and maintained in EBSS (Gibco) at low temperature until manipulation. The *sinus venosus* was resected from the embryos and transfected in hanging drops (Bonet et al., 2015; Dueñas et al., 2020) with microRNA mimics, including miR-23b, miR-130a, miR-106a, and miR-100 precursors, for 24 h at 37°C.

Pre-miRNAs transfection was carried out with Lipofectamine 2000 (Invitrogen) following the manufacturer's instructions. Negative control explants were treated only with Lipofectamine and were run in parallel.

RNA Isolation and qRT-PCR

Samples obtained from H9c2 cells and *sinus venosus* explants after microRNA transfections and control samples were subjected to qRT-PCR analysis following MIQE guidelines (Bustin et al., 2009; Bonet et al., 2015; Lozano-Velasco et al., 2015). RNA was extracted and purified by using a ReliaPrep RNA Cell Miniprep System Kit (Promega) according to the manufacturer's instructions. For mRNA expression measurements, 1 µg of total RNA was used for retro-transcription with a Maxima First Strand cDNA Synthesis Kit for qRT-PCR (Thermo Scientific). Real-time PCR experiments were performed with 2 µL of cDNA, Go Taq qPCR Master Mix (Promega), and corresponding primer sets (**Supplementary Table S2**). For microRNA expression analyses, 20 ng of total RNA was used for retro-transcription with a universal cDNA Synthesis Kit II (Exiqon), and the resulting cDNA was diluted 1/80. Real-time PCR experiments were performed with 1 µL of diluted cDNA and Go Taq qPCR Master Mix (Promega) as well. All qPCRs were performed using a CFX384TM thermocycler (Bio-Rad) following the manufacturer's recommendations. The relative expression of each gene was calculated by using *Gusb* and *Gadph* as internal controls for mRNA expression analyses and *5S* and *6U* for microRNA expression analyses, respectively (Livak and Schmittgen, 2001). Each PCR reaction was carried out in triplicate and repeated in at least three distinct biological samples to obtain representative means. qPCR data were analyzed using $\Delta\Delta\text{Ct}$ (Deepak et al., 2007).

Amplification of Hox Genes From *Sinus Venosus* cDNA at Stages HH11–HH15

CDNA from the *sinus venosus* at stages HH11 and HH15 was obtained and processed as described above. For mRNA expression detection, Dream Taq polymerase (2x) and specific primers (**Supplementary Table S2**) were used, taking *Gapdh* as the internal loading control.

Luciferase Assays of 3'UTRs Hox Genes

Hoxa1 and *Hoxa4* 3'UTR constructs were PCR-amplified from chicken genomic DNA using primers bearing *SpeI*/*HindIII* restriction sites and cloned into the pGLuc-Basic vector (New England BioLabs). 3T3 fibroblasts (ATCC) were co-transfected with 100 ng of the *Hoxa1* and *Hoxa4* luciferase vector, 300 ng of pLuc vector control for internal normalization, and 20 nM of each microRNA. Luciferase activity was measured at 24 h after transfection (Pierce™ Gaussia Luciferase Flash Assay Kit) and normalized to the pLuc vector control (Pierce™ Cypridina Luciferase Flash Assay Kit). Luciferase activity was compared to non-transfected controls. Each luciferase assay was carried out in triplicate and repeated in at least three distinct biological samples to obtain representative assays.

Statistical Analysis

Student's *t*-test was used. Significance levels or *p*-values are stated in each corresponding figure, $p < 0.05$ being considered as statistically significant.

DATA AVAILABILITY STATEMENT

The original contributions presented in the study are included in the article/**Supplementary Materials**, further inquiries can be directed to the corresponding author.

ETHICS STATEMENT

Experimental protocols with animals were performed in agreement with the Spanish law in application of the EU Guidelines for animal research, and conformed to the Guide for the Care and Use of Laboratory Animals, published by the US National Institutes of Health (NIH Publication no.85-23). Approval by the University of Extremadura bioethics board was obtained prior to the initiation of the study.

AUTHOR CONTRIBUTIONS

The experimental study was designed and supervised by CL-S, DF, and VG-M, who also wrote the manuscript. CG-P, AD, and VG-L have contributed to the conception and design of the study, performed the experiments, and analyzed the data. All authors have contributed to the experimental work and analyzed and discussed the results. Also, all authors contributed to manuscript revision, and read and approved the submitted version.

FUNDING

This work has been financed with research grants IB18123 (to CL-S) and GR18185 (to VG-M, CTS005) from the Junta de Extremadura, with FEDER co-financing, and CTS-446 (to DF and AA) from the Junta de Andalucía Regional Council.

ACKNOWLEDGMENTS

We thank Laura Ortega Bermejo for her invaluable technical support with embryo handling and sample preparation for *in situ* hybridization.

SUPPLEMENTARY MATERIAL

The Supplementary Material for this article can be found online at: <https://www.frontiersin.org/articles/10.3389/fcell.2021.767954/full#supplementary-material>

REFERENCES

- Abu-Issa, R., and Kirby, M. L. (2008). Patterning of the Heart Field in the Chick. *Developmental Biol.* 319, 223–233. doi:10.1016/j.ydbio.2008.04.014
- Aguirre, A., Montserrat, N., Zschigna, S., Nivet, E., Hishida, T., Krause, M. N., et al. (2014). *In Vivo* activation of a Conserved microRNA Program Induces Mammalian Heart Regeneration. *Cell Stem Cell* 15, 589–604. doi:10.1016/j.stem.2014.10.003
- Barak, H., Preger-Ben Noon, E., and Reshef, R. (2012). Comparative Spatiotemporal Analysis of Hox Gene Expression in Early Stages of Intermediate Mesoderm Formation. *Dev. Dyn.* 241, 1637–1649. doi:10.1002/dvdy.23853
- Bertrand, N., Roux, M., Ryckebusch, L., Niederreither, K., Dollé, P., Moon, A., et al. (2011). Hox Genes Define Distinct Progenitor Sub-domains within the Second Heart Field. *Developmental Biol.* 353, 266–274. doi:10.1016/j.ydbio.2011.02.029
- Bhatlekar, S., Viswanathan, V., Fields, J. Z., and Boman, B. M. (2017). Overexpression of HOXA4 and HOXA9 Genes Promotes Self-renewal and Contributes to colon Cancer Stem Cell Overpopulation. *J. Cell Physiol* 233, 727–735. doi:10.1002/jcp.25981
- Bonet, F., Dueñas, Á., López-Sánchez, C., García-Martínez, V., Aránega, A. E., and Franco, D. (2015). MiR-23b and miR-199a Impair Epithelial-To-Mesenchymal Transition during Atrioventricular Endocardial Cushion Formation. *Dev. Dyn.* 244, 1259–1275. doi:10.1002/dvdy.24309
- Boureira Oumarou, D., Ji, H., Xu, J., Li, S., Ruan, W., Xiao, F., et al. (2019). Involvement of microRNA-23b-5p in the Promotion of Cardiac Hypertrophy and Dysfunction via the HMGB2 Signaling Pathway. *Biomed. Pharmacother.* 116, 108977. doi:10.1016/j.biopha.2019.108977
- Branco, A. F., Pereira, S. P., Gonzalez, S., Gusev, O., Rizvanov, A. A., and Oliveira, P. J. (2015). Gene Expression Profiling of H9c2 Myoblast Differentiation towards a Cardiac-like Phenotype. *PLoS One* 10, e0129303. doi:10.1371/journal.pone.0129303
- Buckingham, M., Meilhac, S., and Zaffran, S. (2005). Building the Mammalian Heart from Two Sources of Myocardial Cells. *Nat. Rev. Genet.* 6, 826–835. doi:10.1038/nrg1710
- Bustin, S. A., Benes, V., Garson, J. A., Hellemans, J., Huggett, J., Kubista, M., et al. (2009). The MIQE Guidelines: Minimum Information for Publication of Quantitative Real-Time PCR Experiments. *Clin. Chem.* 55, 611–622. doi:10.1373/clinchem.2008.112797
- Camp, E., Dietrich, S., and Münsterberg, A. (2012). Fate Mapping Identifies the Origin of SHF/AHF Progenitors in the Chick Primitive Streak. *PLoS One* 7, e51948. doi:10.1371/journal.pone.0051948
- Cao, L., Kong, L.-P., Yu, Z.-B., Han, S.-P., Bai, Y.-F., Zhu, J., et al. (2012). microRNA Expression Profiling of the Developing Mouse Heart. *Int. J. Mol. Med.* 30, 1095–1104. doi:10.3892/ijmm.2012.1092
- Carmona, R., Ariza, L., Cañete, A., and Muñoz-Chápuli, R. (2018). Comparative Developmental Biology of the Cardiac Inflow Tract. *J. Mol. Cell Cardiol.* 116, 155–164. doi:10.1016/j.yjmcc.2018.02.004
- Cheng, S., Qian, F., Huang, Q., Wei, L., Fu, Y., and Du, Y. (2018). HOXA4, Down-Regulated in Lung Cancer, Inhibits the Growth, Motility and Invasion of Lung Cancer Cells. *Cell Death Dis* 9, 465. doi:10.1038/s41419-018-0497-x
- Chinchilla, A., Lozano, E., Daimi, H., Esteban, F. J., Crist, C., Aranega, A. E., et al. (2011). MicroRNA Profiling during Mouse Ventricular Maturation: a Role for miR-27 Modulating Mef2c Expression. *Cardiovasc. Res.* 89, 98–108. doi:10.1093/cvr/cvq264
- Choi, E., Choi, E., and Hwang, K. C. (2013). MicroRNAs as Novel Regulators of Stem Cell Fate. *Wjsc* 5, 172–187. doi:10.4252/wjsc.v5.i4.172
- Christoffels, V. M., Mommersteeg, M. T. M., Trowe, M.-O., Prall, O. W. J., de Gier-de Vries, C., Soufan, A. T., et al. (2006). Formation of the Venous Pole of the Heart from an Nkx2-5-Negative Precursor Population Requires Tbx18. *Circ. Res.* 98, 1555–1563. doi:10.1161/01.RES.0000227571.84189.65
- Darnell, D. K., Kaur, S., Stanislaw, S., Konieczka, J. K., Yatskevich, T. A., and Antin, P. B. (2006). MicroRNA Expression during Chick Embryo Development. *Dev. Dyn.* 235, 3156–3165. doi:10.1002/dvdy.20956
- De Bono, C., Thellier, C., Bertrand, N., Sturny, R., Jullian, E., Cortes, C., et al. (2018b). T-box Genes and Retinoic Acid Signaling Regulate the Segregation of Arterial and Venous Pole Progenitor Cells in the Murine Second Heart Field. *Hum. Mol. Genet.* 27, 3747–3760. doi:10.1093/hmg/ddy266
- De Bono, C., Théveniau-Ruissy, M., and Kelly, R. G. (2018a). Cardiac fields and Myocardial Cell Lineages. *Card. fields myocardial Cel. lineages* 4, 23–32. doi:10.1093/med/9780198757269.003.0004
- Dueñas, A., Expósito, A., Muñoz, M. D. M., de Manuel, M. J., Cámara-Morales, A., Serrano-Osorio, F., et al. (2020). MiR-195 Enhances Cardiomyogenic Differentiation of the Proepicardium/septum Transversum by Smurf1 and Foxp1 Modulation. *Sci. Rep.* 10, 9334. doi:10.1038/s41598-020-66325-x
- García-Martínez, V., Darnell, D. K., López-Sánchez, C., Susic, D., Olson, E. N., and Schoenwolf, G. C. (1997). State of Commitment of Prospective Neural Plate and Prospective Mesoderm in Late Gastrula/early Neurula Stages of Avian Embryos. *Developmental Biol.* 181, 102–115. doi:10.1006/dbio.1996.8439
- García-Martínez, V., and Schoenwolf, G. C. (1993). Primitive-streak Origin of the Cardiovascular System in Avian Embryos. *Developmental Biol.* 159, 706–719. doi:10.1006/dbio.1993.1276
- Guan, X., Wang, L., Liu, Z., Guo, X., Jiang, Y., Lu, Y., et al. (2016). miR-106a Promotes Cardiac Hypertrophy by Targeting Mitofusin 2. *J. Mol. Cell Cardiol.* 99, 207–217. doi:10.1016/j.yjmcc.2016.08.016
- Hamburger, V., and Hamilton, H. L. (1951). A Series of normal Stages in the Development of the Chick Embryo. *J. Morphol.* 88, 49–92. doi:10.1002/jmor.1050880104
- Hamburger, V., and Hamilton, H. L. (1992). A Series of normal Stages in the Development of the Chick Embryo. *Dev. Dyn.* 195, 231–272. doi:10.1002/aja.1001950404
- Harvey, R. P. (2002). Patterning the Vertebrate Heart. *Nat. Rev. Genet.* 3, 544–556. doi:10.1038/nrg843
- Hochgreb, T., Linhares, V. L., Menezes, D. C., Sampaio, A. C., Yan, C. Y. I., Cardoso, W. V., et al. (2003). A Caudorostral Wave of RALDH2 Conveys Anteroposterior Information to the Cardiac Field. *Development* 130, 5363–5374. doi:10.1242/dev.00750
- Kalayinia, S., Arjmand, F., Maleki, M., Malakootian, M., and Singh, C. P. (2021). MicroRNAs: Roles in Cardiovascular Development and Disease. *Cardiovasc. Pathol.* 50, 107296. doi:10.1016/j.carpath.2020.107296
- Kim, G. H., Samant, S. A., Earley, J. U., and Svensson, E. C. (2009). Translational Control of FOG-2 Expression in Cardiomyocytes by microRNA-130a. *PLoS One* 4, e6161. doi:10.1371/journal.pone.0006161
- Lescroart, F., and Zaffran, S. (2018). Hox and Tale Transcription Factors in Heart Development and Disease. *Int. J. Dev. Biol.* 62, 837–846. doi:10.1387/ijdb.180192sz
- Livak, K. J., and Schmittgen, T. D. (2001). Analysis of Relative Gene Expression Data Using Real-Time Quantitative PCR and the 2- $\Delta\Delta$ CT Method. *Methods* 25, 402–408. doi:10.1006/meth.2001.1262
- López-Sánchez, C., Franco, D., Bonet, F., García-López, V., Aranega, A., and García-Martínez, V. (2015a). Negative Fgf8-Bmp2 Feed-Back Is Regulated by miR-130 during Early Cardiac Specification. *Developmental Biol.* 406, 63–73. doi:10.1016/j.ydbio.2015.07.007
- López-Sánchez, C., Franco, D., Bonet, F., García-López, V., Aranega, A., and García-Martínez, V. (2015b). Reciprocal Repression between Fgf8 and miR-133 Regulates Cardiac Induction through Bmp2 Signaling. *Data in Brief* 5, 59–64. doi:10.1016/j.dib.2015.08.009
- López-Sánchez, C., García-López, V., Schoenwolf, G. C., and García-Martínez, V. (2018). From Epiblast to Mesoderm: Elaboration of a Fate Map for Cardiovascular Progenitors. 3, 14–22. doi:10.1093/med/9780198757269.003.0003
- López-Sánchez, C., and García-Martínez, V. (2011). Molecular Determinants of Cardiac Specification. *Cardiovasc. Res.* 91, 185–195. doi:10.1093/cvr/cvq127
- López-Sánchez, C., García-Martínez, V., and Schoenwolf, G. C. (2001). Localization of Cells of the Prospective Neural Plate, Heart and Somites within the Primitive Streak and Epiblast of Avian Embryos at Intermediate Primitive-Streak Stages. *Cells Tissues Organs* 169, 334–346. doi:10.1159/000047900
- López-Sánchez, C., García-Masa, N., Gañan, C. M., and García-Martínez, V. (2009). Movement and Commitment of Primitive Streak Precardiac Cells during Cardiogenesis. *Int. J. Dev. Biol.* 53, 1445–1455. doi:10.1387/ijdb.072417cl
- López-Sánchez, C., Puelles, L., García-Martínez, V., and Rodríguez-Gallardo, L. (2005). Morphological and Molecular Analysis of the Early Developing Chick Requires an Expanded Series of Primitive Streak Stages. *J. Morphol.* 264, 105–116. doi:10.1002/jmor.10323

- Lozano-Velasco, E., Galiano-Torres, J., Jodar-Garcia, A., Aranega, A. E., and Franco, D. (2015). miR-27 and miR-125 Distinctly Regulate Muscle-Enriched Transcription Factors in Cardiac and Skeletal Myocytes. *Biomed. Res. Int.* 2015, 1–6. doi:10.1155/2015/391306
- Makki, N., and Capecchi, M. R. (2010). Hoxa1 Lineage Tracing Indicates a Direct Role for Hoxa1 in the Development of the Inner Ear, the Heart, and the Third Rhombomere. *Developmental Biol.* 341, 499–509. doi:10.1016/j.ydbio.2010.02.014
- Mommersteeg, M. T. M., Domínguez, J. N., Wiese, C., Norden, J., de Gier-de Vries, C., Burch, J. B. E., et al. (2010). The Sinus Venosus Progenitors Separate and Diversify from the First and Second Heart fields Early in Development. *Cardiovasc. Res.* 87, 92–101. doi:10.1093/cvr/cvq033
- Niederreither, K., Subbarayan, V., Dollé, P., and Chambon, P. (1999). Embryonic Retinoic Acid Synthesis Is Essential for Early Mouse post-implantation Development. *Nat. Genet.* 21 (21), 444–448. doi:10.1038/7788
- Niederreither, K., Vermot, J., Messadeg, N., Schuhbauer, B., Chambon, P., and Dollé, P. (2001). Embryonic Retinoic Acid Synthesis Is Essential for Heart Morphogenesis in the Mouse. *Development* 128 (128), 1019–1031. doi:10.1242/dev.128.7.1019
- Packer, A. I., Crotty, D. A., Elwell, V. A., and Wolgemuth, D. J. (1998). Expression of the Murine Hoxa4 Gene Requires Both Autoregulation and a Conserved Retinoic Acid Response Element. *Development* 125, 1991–1998. doi:10.1242/dev.125.11.1991
- Packer, A. I., Mailutha, K. G., Ambrozewicz, L. A., and Wolgemuth, D. J. (2000). Regulation of the Hoxa4 and Hoxa5 Genes in the Embryonic Mouse Lung by Retinoic Acid and TGFbeta1: Implications for Lung Development and Patterning. *Dev. Dyn.* 217 (217), 62–74. doi:10.1002/(SICI)109710.1002/(SICI)1097-0177(200001)217:1<62:AID-DVDY6>3.0.CO;2-U
- Pang, J. K. S., Phua, Q. H., and Soh, B.-S. (2019). Applications of miRNAs in Cardiac Development, Disease Progression and Regeneration. *Stem Cell Res. Ther.* 10, 336. doi:10.1186/s13287-019-1451-2
- Rajabi, H., Aslani, S., Abhari, A., and Sanajou, D. (2020). Expression Profiles of microRNAs in Stem Cells Differentiation. *Cpb* 21, 906–918. doi:10.2174/138920102166620021909252
- Redkar, A., Montgomery, M., and Litvin, J. (2001). Fate Map of Early Avian Cardiac Progenitor Cells. *Development* 128, 2269–2279. doi:10.1242/dev.128.12.2269
- Roux, M., Laforest, B., Capecchi, M., Bertrand, N., and Zaffran, S. (2015). Hoxb1 Regulates Proliferation and Differentiation of Second Heart Field Progenitors in Pharyngeal Mesoderm and Genetically Interacts with Hoxa1 during Cardiac Outflow Tract Development. *Developmental Biol.* 406, 247–258. doi:10.1016/j.ydbio.2015.08.015
- Roux, M., and Zaffran, S. (2016). Hox Genes in Cardiovascular Development and Diseases. *Jdb* 4, 14. doi:10.3390/jdb4020014
- Ryckebusch, L., Wang, Z., Bertrand, N., Lin, S.-C., Chi, X., Schwartz, R., et al. (2008). Retinoic Acid Deficiency Alters Second Heart Field Formation. *Proc. Natl. Acad. Sci.* 105, 2913–2918. doi:10.1073/pnas.0712344105
- S.A. Deepak, S., K.R. Kottapalli, K., R. Rakwal, R., G. Oros, G., K.S. Rangappa, K., H. Iwahashi, H., et al. (2007). Real-Time PCR: Revolutionizing Detection and Expression Analysis of Genes. *Cg* 8 (4), 234–251. doi:10.2174/138920207781386960
- Schultheiss, T. M., Xydas, S., and Lassar, A. B. (1995). Induction of Avian Cardiac Myogenesis by Anterior Endoderm. *Development* 121, 4203–4214. doi:10.1242/dev.121.12.4203
- Searcy, R. D., and Yutzey, K. E. (1998). Analysis of Hox Gene Expression during Early Avian Heart Development. *Dev. Dyn.* 213, 82–91. doi:10.1002/(sici)1097-0177(199809)213:1<82:aid-aja8>3.0.co;2-u
- Shu, J., Silva, B. V. R. e., Gao, T., Xu, Z., and Cui, J. (2017). Dynamic and Modularized microRNA Regulation and its Implication in Human Cancers. *Sci. Rep.* 7, 13356. doi:10.1038/s41598-017-13470-5
- Sirbu, I. O., Zhao, X., and Duester, G. (2008). Retinoic Acid Controls Heart Anteroposterior Patterning by Down-regulating Isl1 through the Fgf8 Pathway. *Dev. Dyn.* 237, 1627–1635. doi:10.1002/dvdy.21570
- Stefanovic, S., Laforest, B., Desvignes, J.-P., Lescroart, F., Argiro, L., Maurel-Zaffran, C., et al. (2020). Hox-dependent Coordination of Mouse Cardiac Progenitor Cell Patterning and Differentiation. *Elife* 9, e55124. doi:10.7554/eLife.55124
- Stefanovic, S., and Zaffran, S. (2017). Mechanisms of Retinoic Acid Signaling during Cardiogenesis. *Mech. Development* 143, 9–19. doi:10.1016/j.mod.2016.12.002
- Sticht, C., De La Torre, C., Parveen, A., and Gretz, N. (2018). miRWalk: An Online Resource for Prediction of microRNA Binding Sites. *PLoS One* 13 (10), e0206239. doi:10.1371/journal.pone.0206239
- Sucharov, C., Bristow, M. R., and Port, J. D. (2008). miRNA Expression in the Failing Human Heart: Functional Correlates. *J. Mol. Cell Cardiol.* 45, 185–192. doi:10.1016/j.yjmcc.2008.04.014
- Tarantino, C., Paoletta, G., Cozzuto, L., Minopoli, G., Pastore, L., Parisi, S., et al. (2010). miRNA 34a, 100, and 137 Modulate Differentiation of Mouse Embryonic Stem Cells. *FASEB j.* 24, 3255–3263. doi:10.1096/fj.09-152207
- Thum, T., Catalucci, D., and Bauersachs, J. (2008). MicroRNAs: Novel Regulators in Cardiac Development and Disease. *Cardiovasc. Res.* 79, 562–570. doi:10.1093/cvr/cvn137
- van den Berg, G., Abu-Issa, R., de Boer, B. A., Hutson, M. R., de Boer, P. A. J., Soufan, A. T., et al. (2009). A Caudal Proliferating Growth center Contributes to Both Poles of the Forming Heart Tube. *Circ. Res.* 104, 179–188. doi:10.1161/CIRCRESAHA.108.185843
- van Wijk, B., Barnett, P., and van den Hoff, M. J. B. (2018). The Developmental Origin of Myocardium at the Venous Pole of the Heart. 8, 64–74. doi:10.1093/med/9780198757269.003.0008
- van Wijk, B., van den Berg, G., Abu-Issa, R., Barnett, P., van der Velden, S., Schmidt, M., et al. (2009). Epicardium and Myocardium Separate from a Common Precursor Pool by Crosstalk between Bone Morphogenetic Protein- and Fibroblast Growth Factor-Signaling Pathways. *Circ. Res.* 105, 431–441. doi:10.1161/CIRCRESAHA.109.203083
- Waldo, K. L., Hutson, M. R., Ward, C. C., Zdanowicz, M., Stadt, H. A., Kumiski, D., et al. (2005). Secondary Heart Field Contributes Myocardium and Smooth Muscle to the Arterial Pole of the Developing Heart. *Developmental Biol.* 281, 78–90. doi:10.1016/j.ydbio.2005.02.012
- Wu, S., Huang, S., Ding, J., Zhao, Y., Liang, L., Liu, T., et al. (2010). Multiple microRNAs Modulate p21Cip1/Waf1 Expression by Directly Targeting its 3' Untranslated Region. *Oncogene* 29, 2302–2308. doi:10.1038/onc.2010.34
- Yan, S., and Jiao, K. (2016). Functions of miRNAs during Mammalian Heart Development. *Ijms* 17, 789. doi:10.3390/ijms17050789
- Yang, F., Miao, L., Mei, Y., and Wu, M. (2013). Retinoic Acid-Induced HOXA5 Expression Is Co-regulated by HuR and miR-130a. *Cell Signal.* 25 (25), 1476–1485. doi:10.1016/j.cellsig.2013.03.015
- Zaffran, S., and Kelly, R. G. (2012). New Developments in the Second Heart Field. *Differentiation* 84, 17–24. doi:10.1016/j.diff.2012.03.003

Conflict of Interest: The authors declare that the research was conducted in the absence of any commercial or financial relationships that could be construed as a potential conflict of interest.

Publisher's Note: All claims expressed in this article are solely those of the authors and do not necessarily represent those of their affiliated organizations, or those of the publisher, the editors, and the reviewers. Any product that may be evaluated in this article, or claim that may be made by its manufacturer, is not guaranteed or endorsed by the publisher.

Copyright © 2022 Garcia-Padilla, Dueñas, Franco, Garcia-Lopez, Aranega, Garcia-Martinez and Lopez-Sanchez. This is an open-access article distributed under the terms of the Creative Commons Attribution License (CC BY). The use, distribution or reproduction in other forums is permitted, provided the original author(s) and the copyright owner(s) are credited and that the original publication in this journal is cited, in accordance with accepted academic practice. No use, distribution or reproduction is permitted which does not comply with these terms.